Journal of Magnetic Resonance 216 (2012) 69–77

Contents lists available at SciVerse ScienceDirect

Journal of Magnetic Resonance

journal homepage: www.elsevier.com/locate/jmr

Effect of freezing conditions on distances and their distributions derived from Double Electron Electron Resonance (DEER): A study of doubly-spin-labeled T4 lysozyme

Elka R. Georgieva [a], Aritro S. Roy [a], Vladimir M. Grigoryants [b,1], Petr P. Borbat [a], Keith A. Earle [c,a], Charles P. Scholes [b,1], Jack H. Freed [a,*]

[a] Department of Chemistry and Chemical Biology and ACERT, Cornell University, Ithaca, NY 14853, United States
[b] Department of Chemistry, University at Albany, 1400 Washington Avenue, Albany, NY 12222, United States
[c] Department of Physics, University at Albany, 1400 Washington Avenue, Albany, NY 12222, United States

ARTICLE INFO

Article history:
Received 22 June 2011
Revised 10 January 2012
Available online 24 January 2012

Keywords:
Double Electron Electron Resonance (DEER)
Pulse dipolar spectroscopy (PDS)
T4 lysozyme
Bi-label distance
Bi-label distance distribution
Freezing perturbation
Rapid freeze quench

ABSTRACT

Pulsed dipolar ESR spectroscopy, DEER and DQC, require frozen samples. An important issue in the biological application of this technique is how the freezing rate and concentration of cryoprotectant could possibly affect the conformation of biomacromolecule and/or spin-label. We studied in detail the effect of these experimental variables on the distance distributions obtained by DEER from a series of doubly spin-labeled T4 lysozyme mutants. We found that the rate of sample freezing affects mainly the ensemble of spin-label rotamers, but the distance maxima remain essentially unchanged. This suggests that proteins frozen in a regular manner in liquid nitrogen faithfully maintain the distance-dependent structural properties in solution.

We compared the results from rapidly freeze-quenched ($\leqslant$100 μs) samples to those from commonly shock-frozen (slow freeze, 1 s or longer) samples. For all the mutants studied we obtained inter-spin distance distributions, which were broader for rapidly frozen samples than for slowly frozen ones. We infer that rapid freezing trapped a larger ensemble of spin label rotamers; whereas, on the time-scale of slower freezing the protein and spin-label achieve a population showing fewer low-energy conformers. We used glycerol as a cryoprotectant in concentrations of 10% and 30% by weight. With 10% glycerol and slow freezing, we observed an increased slope of background signals, which in DEER is related to increased local spin concentration, in this case due to insufficient solvent vitrification, and therefore protein aggregation. This effect was considerably suppressed in slowly frozen samples containing 30% glycerol and rapidly frozen samples containing 10% glycerol. The assignment of bimodal distributions to tether rotamers as opposed to protein conformations is aided by comparing results using MTSL and 4-Bromo MTSL spin-labels. The latter usually produce narrower distance distributions.

1. Introduction

Pulse dipolar spectroscopy (PDS) of paramagnetic nitroxide bi-labels has found increasingly wide use for obtaining distances and distance distributions between bi-labeled sites in biological macromolecules. Combined with site-directed spin-labeling (SDSL) [1], Double Electron Electron Resonance (DEER), for example, has provided a highly sensitive method for measuring distances in the range of 2–8.7 nm [2–4]. Interlabel distance distributions are obtained from the time domain signal by the Tikhonov regularization method [5] with further refinement possible by maximum entropy methods [6]. The nitroxide spin-labels are small and generally non-perturbing to the function of the biomacromolecule. The combination of PDS and SDSL has been notably useful on macromolecular systems which are not amenable to more traditional crystallographic and NMR structural determinations, such as inherently disordered [7,8] and large, multisubunit macromolecules [9–11]. Thus, the growing interest in the method requires detailed knowledge about the possible perturbations, which can be introduced by experimental variables, such as sample preparation and handling.

Here we focus on the effect of sample freezing and concentration of the cryoprotectant, glycerol, on the distance distribution, P(r), between spin-labels attached to water-exposed residues in

* Corresponding author.
E-mail addresses: erg54@cornell.edu (E.R. Georgieva), as836@cornell.edu (A.S. Roy), grigor@albany.edu (V.M. Grigoryants), ppb@ccmr.cornell.edu (P.P. Borbat), kearle@albany.edu (K.A. Earle), CPS14@Albany.edu (C.P. Scholes), jhf3@cornell.edu (J.H. Freed).
[1] Fax: +1 518 442 3462.

1090-7807/$ - see front matter © 2012 Elsevier Inc. All rights reserved.
doi:10.1016/j.jmr.2012.01.004

T4 lysozyme (T4L). PDS experiments require frozen samples since they are typically performed at cryogenic temperatures, usually below 70 K. Thus, questions arise about freezing-induced perturbation to distance distributions. Even for the arguably rigid structures found in well-defined globular proteins, PDS usually produces distance distributions between the nitroxide moieties of bi-labeled molecules with broadening that may arise from various rotamers of the spin-label tether [12,13] and from conformational substates of the macromolecule. Both the rotamer and conformational distributions may, in principle, be perturbed by the method of freezing.

We provide in this work specific instances of how the freezing protocol may affect the distance distributions derived from DEER. We compare the results from bi-labeled samples prepared in a regular shock-freezing procedure, which we refer to as 'slow freezing', where slow freezing occurs in a time of 1 s or longer with the results from very fast rapid freezing which occurs on a 100 μs (or possibly shorter) time scale. Since glycerol cryoprotectant has normally been used as a vitrifying agent to prevent excluded volume effects resulting in formation of large water crystals and solute segregation/aggregation, we also compared distances and distance distributions from frozen bi-labeled samples under slow (1 s) freezing conditions at 10% and 30% (by weight) glycerol. To the authors' knowledge, no such investigation aimed at the expanding field of pulse dipolar spectroscopy has been done to measure the perturbation from freezing.

The choice of T4L as a model system for our experiments was based on the properties of this protein: T4L is a small globular protein of 164 amino acids with predominantly helical structure and small regions of beta-sheets as revealed by crystallography [14] (Fig. 1). It has been the paradigm protein for ESR with mutation protocols well worked out. ESR-SDSL studies have been directed both at ambient temperature to reflect the dynamic locale of the spin label [1,15–17] and at low temperature to determine by PDS the distances between bi-label sites [18]. Because of its relatively rigid structure, T4L usually produces sharp distance distributions from the well defined dipolar oscillations that last for several microseconds in the DEER time-domain signals. For the present work a set of double cysteine mutants of T4L were produced, that are 8C/44C, 8C/128C, 65C/128C, and 65C/135C (Fig. 1), which include residues either within the same domain or residues in both N-terminal and C-terminal domains [19]. Both MTSL and its bromo-derivative have been used to help to distinguish rotamer effects on P(r).

Our major findings suggest that the procedure of sample freezing for PDS in general does not introduce perturbations into the protein structure/properties since we observed virtually the same inter-spin distance maxima for slowly and rapidly frozen samples. The freezing rate affects predominantly the population of spin-label conformers, and therefore their distance distributions. For the slowly frozen samples, in a regular shock-freeze procedure, the concentration of glycerol affects the efficiency of vitrification and consequently the homogeneous distribution of protein molecules within the sample volume. Thus, at 10% glycerol we observed shortened phase memory relaxation time (T_m) and lowered signal-to-noise ratio (SNR) of the DEER signal because of increased local concentration of spin-labeled protein. For rapidly frozen samples in 10% glycerol the protein did not have such a tendency to aggregate, and the spin-labels had longer T_m's and gave greater SNR's for the time-dependent DEER amplitude. Therefore, rapid freezing of samples with lower concentration of glycerol might be a useful technique to preserve the properties of proteins and obtain DEER signals of high quality. We also find that the use of the bromo-derivative of MTSL usually leads to a narrower P(r).

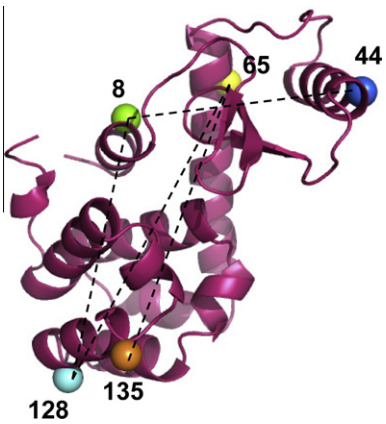

Fig. 1. A cartoon representation of the T4L structure, PDB code 3LZM [19]. The C_β atoms of the residues, which were mutated to cysteines and spin-labeled, are shown as colored spheres and labeled by the number of the residue. The doubly spin labeled residues, which were used for distance measurements are connected by dotted lines.

2. Experimental section

2.1. Mutagenesis, protein expression, purification and spin-labeling

Proteins used in this study were produced from the ampicillin-resistant plasmid (obtained from AddGene, plasmid #18111) carrying the gene for cysteine-free WT* T4L, developed in the laboratory of Matsumura [20]. We designed four double cysteine mutants, 8C/44C, 8C/128C, 65C/128C, and 65C/135C, and generated them by site-directed mutagenesis using the Quick-Exchange Multi Site-Directed Mutagenesis Kit (Agilent Technologies, Stratagene Products Division), as instructed by manufacturer. After confirming the successful mutations by DNA sequencing, we transferred the plasmids into *E. coli* BL21(DE3) cells, and colonies were grown overnight at 37 °C on LB/agar/ampicillin plates. Mutants were expressed at 37 °C in Terrific broth (Fluka) containing 100 μg/ml ampicillin, inoculated with cell stock solutions from single colonies incubated overnight in LB medium at 37 °C. The protein expression was induced by adding Isopropyl-β-D-thiogalactoside (IPTG) to a concentration of 0.75 mM to the cell culture at an OD of 0.8. Cells were harvested within 90 min after the induction and resuspended in a buffer containing 25 mM MOPS, 25 mM Tris, 1 mM DTT (Dithiothreitol), 1 mM PMSF (phenylmethylsulfonyl fluoride) and 10% glycerol, pH 7.6. We used sonication on ice to disrupt the bacterial cell wall and release the protein into the buffer. Cell debris was removed by centrifugation, and the supernatants were collected for further purification. The T4L double mutants were purified on CM Sepharose ion exchange resin (Sigma). Two steps of washing with 40 and 100 mM NaCl were applied, and the protein was eluted with 220 mM NaCl. The eluted T4L was analyzed by SDS–PAGE, and a single band was observed at about 18 kDa, the molecular weight corresponding to the weight of T4L (data not shown).

The purified double mutants of T4L were spin labeled with a 10-fold excess of either MTSL ((1-Oxyl-2,2,5,5-tetramethyl-Δ3-pyrroline-3-methyl) Methanethiosulfonate) or 4-Bromo-MTSL (4-Bromo-(1-oxyl-2,2,5,5-tetramethyl-Δ3-pyrroline-3-methyl) Methanethiosulfonate) (Toronto Research Chemicals, Inc.) in a buffer containing 25 mM MOPS, 25 mM Tris, 50 mM NaCl and 10% glycerol, pH 7.6, used thereafter as the final buffer composition. The spin-labeling was carried out for 2 h at room temperature and continued overnight at 4 °C. The unreacted spin-label was removed by washing the protein solutions in centrifuge concentrators, 5 kDa cutoff. The final samples for each T4L mutant, prior to pulsed dipolar measurements, were prepared in both regular buffer with ddH_2O/glycerol and with 90% D_2O/glycerol-d8. All data

shown in this paper were obtained in buffer with 90% D_2O. Protein concentration was in the range of 30–80 μM. No difference in the DEER signals and reconstructed distances was observed from protein in buffer containing H_2O/glycerol or D_2O/glycerol-d8, keeping all other conditions unchanged (data not shown). However, for samples with H_2O buffer, shorter transient evaluation times occurred because there was a shortened phase memory relaxation and a faster decay in the spin echo amplitude. We recorded the spin-labeling efficiency at or close to 100% for all T4L mutants, as estimated by comparing the concentration of spins to a nitroxide radical standard [8]. The protein concentration was determined by measuring UV absorbance at 280 nm using a calculated extinction coefficient of $\varepsilon = 24750\ M^{-1}\ cm^{-1}$ (protein properties calculator Scripps Research Institute).

2.2. DEER distance measurements

All measurements were done using a 17.3 GHz home-built Ku-band pulse spectrometer [21,22] at 60 K. A standard 4-pulse DEER sequence was used with π/2-π-π pulse widths of 16 ns, 32 ns and 32 ns, respectively, and a 32 ns π pump pulse was used. The frequency separation between detection and pump pulses was 70 MHz. The detection pulses were positioned at the low-field edge and the pump pulse was positioned near the center of nitroxide spin-label spectrum, close to the maximum. Distances measured were in the range of 3–5 nm, and the DEER evolution time periods (t_m) used were from 3 to 7 μs covering at least 2.5 periods of dipolar oscillations for each case. The homogeneous background was removed from the raw time-domain DEER signals and the distances were reconstructed from the base-line corrected and normalized signals by using the Tikhonov regularization (*L*-curve) method [5] and refined by the Maximum Entropy Method (MEM) [6] (examples with detailed procedure of DEER signals processing and distance reconstruction are given in Supplementary data).

2.3. Freezing methods

To study the effect of sample freezing on the DEER signal and on its reconstructed distances and distance distributions, we used three different methods of freezing as follows: (1) Rapid freezing (RF) was achieved by on the sub 100 μs time scale by spraying a rapid, fine jet of sample onto a cryogenic metal surface (rapid-freeze quench procedure). The samples prepared in this procedure are referred to as 'rapidly frozen'; (2) Slow freezing (SF) occurred on the time scale of 1.5 s and was achieved in a regular shock-freezing procedure by plunging the ESR sample tube into liquid nitrogen The samples prepared in this procedure are referred to as 'slowly frozen'; (3) Very slow freezing (VSF) was achieved over a period of 30–40 s by placing the ESR sample tube into an empty 250 mL beaker within a −80 °C freezer The samples prepared in this procedure are referred to as 'very slowly frozen'. The freezing techniques are described in more detail in the following sub-sections.

2.3.1. Rapid freezing – (RF)

The micromixer for rapid freeze-quench was fabricated at the Cornell Nanofabrication Facility. The device was used here simply for rapid freezing rather than for kinetic mixing followed by rapid freezing. The size of its outlet [23] was approximately ($10\ \mu m \times 100\ \mu m = 1000\ \mu m^2$), the flow velocity was 50 M/s, and the delivery time from mixer outlet to cryowheels was 500 μs. This system achieved rapid freezing by spraying a high velocity jet of sample on rapidly rotating cryogenic (100 K) gold-plated, oxygen free copper wheels. It was fashioned according to plans of Lin et al., [23] whose rapid freeze quench system provided freeze-quenched metalloprotein samples to within ~100 μs of mixing. The frozen sample was removed from the rotating wheels as a fine powder by spring-loaded Teflon scrapers. The powder was swept into a collection funnel within the liquid nitrogen and thence to an ESR tube where it was packed using a Teflon packing stick under liquid nitrogen. Samples of approximately two cm height were packed in quartz tubes (VitroCom, Mountain Lakes, NJ) of 2.0 mm i.d., 2.4 mm o.d. By comparison of the sample height of packed frozen powder to the height of sample after melting, the efficiency of packing was 60%.

We used a rapid reaction, which was the destruction of paramagnetic 1 mM 2,2,6,6-Tetramethylpiperidinyloxy (TEMPO) by 430 mM sodium dithionite, to calibrate the freezing time on the wheel. (this rapid reaction had previously been used to calibrate our ambient temperature, stopped-flow ESR [24,25]). By extrapolating the amplitude of the kinetically decaying signal back to zero time of flight, we determined that the time for freezing on the wheel was 30 μs with an uncertainty of ±70 μs. The deVries group used rapid sample freezing on a cryogenic plate, and by a series of mixers with different output orifice sizes, they calibrated the orifice size vs. freezing time. Their calibration indicates that for a 1000 μm^2 output orifice the actual freezing time on the cryogenic metal would be 100–150 μs (pp. 53–56, [26]). A cryowheel device [27] very similar to ours was developed in the lab of Brian M. Hoffman and was estimated to have a 5 μs freezing time. This 5 μs estimate was obtained from formulas and graphs developed by Bald [28] and Jones [29] to estimate the rapid freezing time of a thin tissue layer on a cryogenic metal block; this approach requires knowledge of the low temperature sample specific heat, thermal conductivity, and thickness. In combining our own estimates with those of others, we would put an upper limit of 100 μs to the freezing time on the cryowheel. However, the critical issue here may not be the freezing time *per se* but the facility of the rapid freeze quench method to prevent formation of ice crystals and segregation of solute, possibly by rapid formation of amorphous ice.

2.3.2. Slow freezing (SF)

In ordinary or slow freezing, the ESR-tube containing the sample solution was dipped into liquid nitrogen and shaken vigorously until the sample was frozen. The time for heat transfer is limited by slow heat transfer from the sample through the insulating nitrogen vapor layer on the surface of the sample tube. The freezing time was estimated by monitoring with a fast electronic data logger the voltage of a thermocouple immersed in the sample tube during the freezing procedure. The 10% glycerol solution froze at −3 °C and the time for freezing to occur at this temperature was approximately 1.3 s. It took about 3 s for the sample temperature to decrease from room temperature to −3 °C.

2.3.3. Very slow freezing (VSF)

In order to let the sample freeze over a longer time, we placed the ESR-tube containing the sample in a −80 °C refrigerator. This method is not highly advisable for biological samples as the solute may precipitate. In cooling from room temperature the VSF sample reproducibly supercooled to about −12 °C within 150 s and then its temperature rapidly jumped back to the −3 °C freezing temperature, where it froze within 30–40 s.

2.4. Percentage of glycerol, vitrifying agent

For an experimentally consistent comparison of results from rapid freeze, slow freeze and very slow freeze, 10% glycerol (weight) were used. (It should be noted that 10% glycerol is not a necessity for very rapid freezing because good powders can be obtained with no glycerol.) For rapid freezing, 30% glycerol makes the solution sufficiently viscous that the pressures needed to achieve rapid flow could cause breakage of the mixer assembly. For a comparison of the effects of glycerol on slow freezing results, samples

with either 10% or 30% glycerol were used and the results were compared keeping all other experimental parameters the same. The ordinary slow frozen samples with 30% glycerol appear transparent, whereas the samples with only 10% glycerol are white in color. All ESR data reported in this study were obtained from samples containing glycerol-d8 and D_2O.

Two samples of 100 μM Tempol (4-Hydroxy TEMPO) in 30% or 50% (by weight) glycerol-d8/D_2O were slowly frozen and their DEER signals were collected under the same experimental condition as for samples of T4L doubly spin-labeled mutants.

3. Results

3.1. Effect of freezing rate on pulse-DEER signal and distance distributions for doubly spin-labeled with MTSL T4L mutant

For all mutants we observed broadening in the distance distributions when the samples were prepared by rapid freezing, as compared to the distance distributions from slowly frozen samples. Besides the overall broadening of fast frozen samples, fast freezing resulted also in changes in the relative intensities of components in distance distributions. Although the rapid and slow freezing altered the fine structures of the distance distributions, the distance maxima corresponding to the most probable distance between spin-labels remained virtually unchanged. In Fig. 2 (right panels) we compare the distance distributions for all four doubly spin-labeled mutants of T4L, 8/44, 8/128, 65/128, and 65/135 from samples which were prepared by either rapid-freeze quench (in green) or slow freezing in liquid nitrogen (in blue), and also very slow freezing at −80 °C (in red for mutant 8/128). All results are from samples containing 10% glycerol.

In detail: (i) The mutant 8/44 after slow freezing gave rise to a sharp peak with maximum at 3.1 nm and two shoulders at shorter and longer distances. The distance distribution from the rapidly frozen sample is broader and also spans longer distances (Fig. 2A); (ii) The most intriguing distance distribution was obtained for doubly spin-labeled mutant 8/128. This particular mutant yielded a bimodal distance distribution with well separated peaks having maxima at 3.7 nm and 4.0 nm when frozen slowly (Fig. 2B). The very slowly frozen sample (frozen over 30 s or more) showed the sharpest features in the distance distribution. However, the two peaks of 8/128 mutant are merged into one broad peak with the rapidly frozen sample; (iii) The inter-spin distances from slowly frozen mutant 65/128 showed a sharp peak with a maximum at 4.8 nm and a shoulder at 4.4 nm, and again, general broadening with a relative increase in the intensity of its peak at 4.4 nm with respect to the peak at 4.8 nm when rapid-frozen (Fig. 2C); (iv) The slowly frozen 65/135 mutant showed primarily a sharp peak at 4.6 nm with a shoulder at 4.2 nm, while its rapidly frozen counterpart was broadened overall and showed a more intense shoulder at 4.2 nm (Fig. 2D).

An interesting observation from this experiment was also the effect of freezing rate on the DEER time-domain signals: The slowly frozen samples with 10% glycerol for all doubly spin-labeled mutants produced time-domain signals with reduced SNR, as compared to signals from rapidly frozen samples with the same content of glycerol (Fig. 2, right panels). We further elaborate on this effect in more detail in the next sections.

3.2. Effect of the concentration of glycerol vitrifying agent (cryoprotectant) on pulse-DEER signal and distance distributions for doubly spin-labeled with MTSL T4L mutant

To better understand how glycerol alters the quality of DEER data and the resultant distance distributions, we used two different concentrations of glycerol, which were 10% and 30%, under slow freezing conditions, and for completeness, we also included a comparison to corresponding rapidly frozen samples containing 10% glycerol. The distance distributions of the slowly frozen 10% and 30% glycerol samples were narrower and similar to each other, while the rapidly frozen distances and distributions were, as already shown in Fig. 2, broader. Raw time-domain DEER, base-line corrected DEER signals, and reconstructed distances are shown in Fig. 3, A, B, C for mutants 8/44, 8/128, and 65/135, respectively. As a function of freezing method, differences are observed in the raw time-domain signals, which are the product of the dipolar signal of the coupled intramolecular spins of interest (V_{intra}) and intermolecular spin–spin interactions with spin-labeled molecules from the surrounding (V_{inter}) [2,3,30]. The latter V_{inter} manifests itself in an exponentially decaying background signal (plotted in gray in Fig. 3A–C, left-most panels), which reports on the local spin-concentration. For slowly frozen samples, we observed a significantly increased slope in the background signal in the raw DEER data when 10% glycerol was used, compared to corresponding samples containing 30% glycerol. Interestingly, when the samples with 10% glycerol were rapidly frozen, they gave raw DEER signals with shallower slopes, comparable to those from slowly frozen samples containing 30% glycerol (Fig. 3A–C, left-most panels). The dipolar signals were extracted by removal of the homogeneous background (the exponential slope due to V_{inter}). Fig. 3A–C, middle panel, shows the similarity of the dipolar signals V_{intra} of the different mutants, where we note that the rapidly frozen samples showed less amplitude in their longer time oscillations (because of the wider breadth of their distance distributions) and the slowly frozen sample in 10% glycerol showed a poorer SNR, because of enhanced intermolecular spin–spin interactions due to protein segregation, resulting into shortened T_m's.

3.3. Rapid vs. slow freezing: effective local spin concentration

To further investigate how to produce a more uniform spin distribution within a sample by rapid-freezing, we performed a control experiment with 100 μM Tempol (4-Hydroxy TEMPO) in 30% and 50% (by weight) glycerol-d8/D_2O: We collected the DEER signal at the same experimental condition as for samples of T4L doubly spin-labeled mutants. Since in the case of Tempol in glycerol/water there are no coupled spins (i.e. there is no V_{intra}), the only contribution to the DEER signal is the interaction with neighboring molecules producing an exponentially decaying slope proportional to the local spin-concentration (Fig. 4A). From this slope we could estimate the local spin concentration and compare it with the actual concentration of Tempol molecules. In DEER the inter-molecular interactions are characterized by the following equation [3,22,31]:

$$V_{inter}(t) = \exp(-kt) \tag{1}$$

with a decay rate per microsecond

$$k^{-1} = 1.0027\frac{10^{-3}}{pC} \tag{2}$$

where C is the molar concentration and p is the probability of flipping B spins by the pumping pulse. For our experimental conditions we found that p is equal to 0.23 from calculations and confirmed by experiment. Therefore the local spin-concentration can be calculated from the slope of the inter-molecular DEER signal. In the case of Tempol in 50% glycerol we obtained a slope of −0.023 per microsecond on a logarithmic scale and calculated a local spin concentration of 100 μM, which corresponds to the actual concentration of Tempol molecules in the sample, and indicates that a fully vitrified glycerol-d8/D_2O mixture provides a homogeneous distribution of

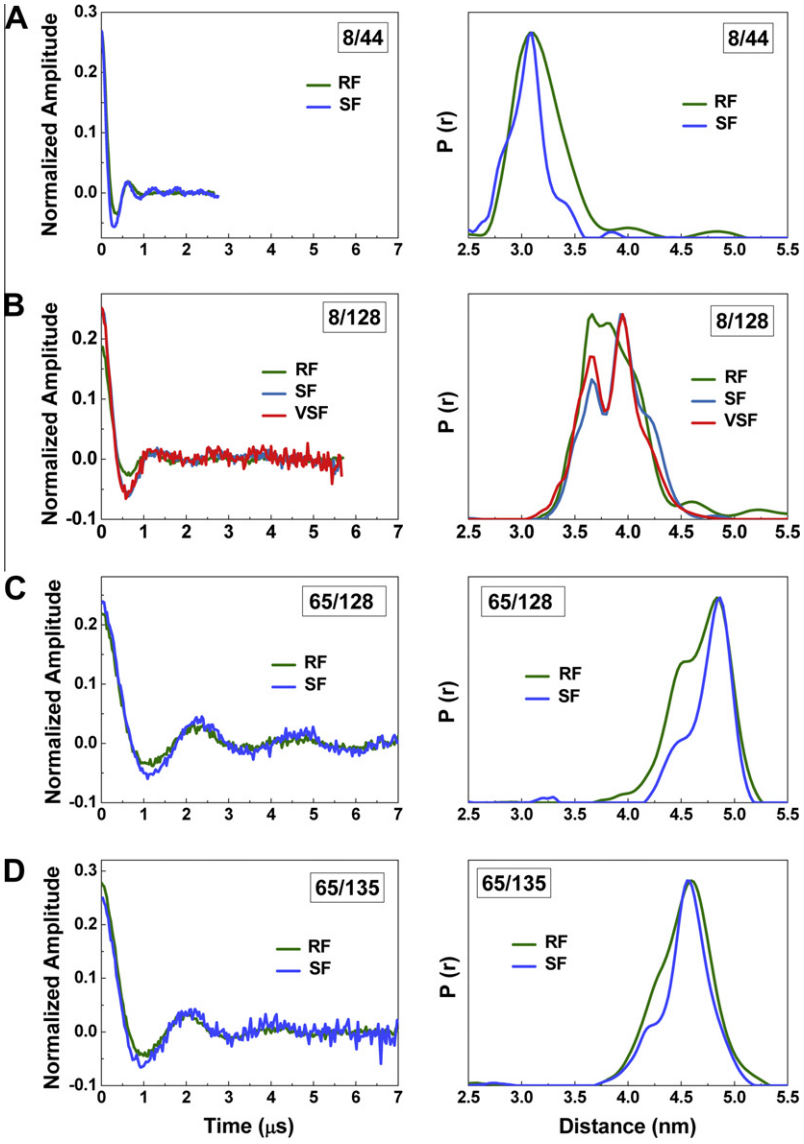

Fig. 2. This figure provides base-line corrected and normalized DEER signals (left) and corresponding reconstructed distances and distance distributions (right) for four bi-spin labeled mutants of T4L. The data labeled (A) are for mutant 8/44; (B) for mutant 8/128; (C) for mutant 65/126; and (D) for mutant 65/135. The DEER signals and distance distributions obtained for rapidly frozen (RF), ⩽100 μs, samples are plotted in green, those for slowly frozen (SF) samples, within 1 s, are in blue, and those for very slowly frozen (VSF) samples, within 1 min or more, are in red. All samples contained 10% glycerol. The distance distributions are normalized to unity at maximum intensity.

solute molecules at cryogenic temperatures. In the case of 30% glycerol we obtained a slope of −0.046 per a microsecond on logarithm scale and calculated a local spin concentration of 200 μM, which is twice the actual concentration of Tempol molecules, indicating inhomogeneity in the distribution of Tempol molecules due to aggregation. Then we compared the slopes which we used to approximate the background signals for T4L samples prepared by rapid freezing in 10% glycerol and those regularly frozen in liquid N_2 in 30% glycerol and we found that rapid freezing decreases the local spin concentration by approximately a factor of 1.5–2, similar to fully vitrified sample of Tempol in 50% glycerol-d8/D_2O, which is shown in Fig. 4B and C for doubly spin-labeled with MTSL mutants 8/128 and 65/135. However, for the samples containing 10% glycerol and frozen in a regular shock-freeze procedure the decay of the background signal was 5–6 times larger than those for rapidly frozen sample in 10% glycerol (Fig. 4B and C). We demonstrate this effect in more detail by using the data for mutant 65C/135C: The slopes of the background signals on logarithm scale were −0.028, −0.057, and −0.133 yielding local spin concentrations of 122 μM, 248 μM, and 578 μM for rapidly frozen sample in 10% glycerol, slowly frozen sample in 30% glycerol and slowly frozen sample in 10% glycerol, respectively. The protein concentration estimated by UV absorbance at 280 nm protein concentration was 56 μM, which is in very good agreement with the local spin concentration in rapidly frozen sample in 10% glycerol for doubly spin-labeled T4L molecules. However, such an agreement could be affected by several sources of error, such as absolute protein concentration determination, presence of unreacted spin-label and others.

3.4. Probing the protein conformation vs. spin-label rotamer conformation: MTSL vs. 4-Bromo MTSL

Since we observed relatively complex distance distributions for all MTSL doubly spin-labeled mutants, it was not obvious whether these distance distributions originate from multiple protein backbone conformations trapped during sample freezing, or whether they reflect just the population of different MTSL rotamers. To answer this question: we spin-labeled three of the T4L mutants,

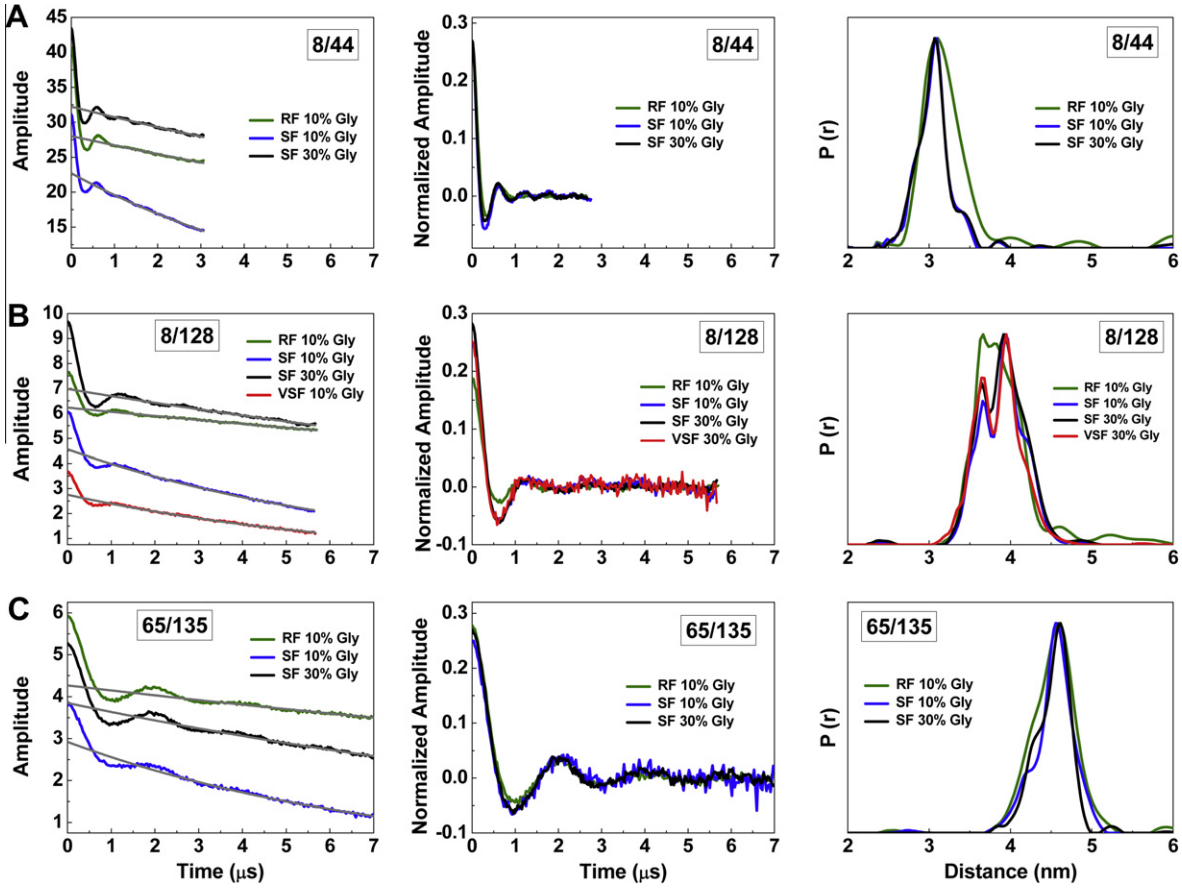

Fig. 3. This figure shows raw time-domain DEER signals together with the best approximation of the homogeneous background (left), base-line corrected (with removed background) and normalized DEER signals (middle) and corresponding reconstructed distances and distance distributions (right) acquired for: (i) slowly frozen (SF) samples containing 10% glycerol (blue), (ii) slowly frozen samples containing 30% glycerol (black), and (iii) rapidly frozen samples (RF) containing 10% glycerol (red). The data are labeled (A) for mutant 8/44; (B) for mutant 8/128, and (C) for mutant 65/135. The data for very slowly frozen sample of mutant 8/128 are also shown in panel B in red. The distance distributions are normalized in arbitrary units to unity at maximum intensity.

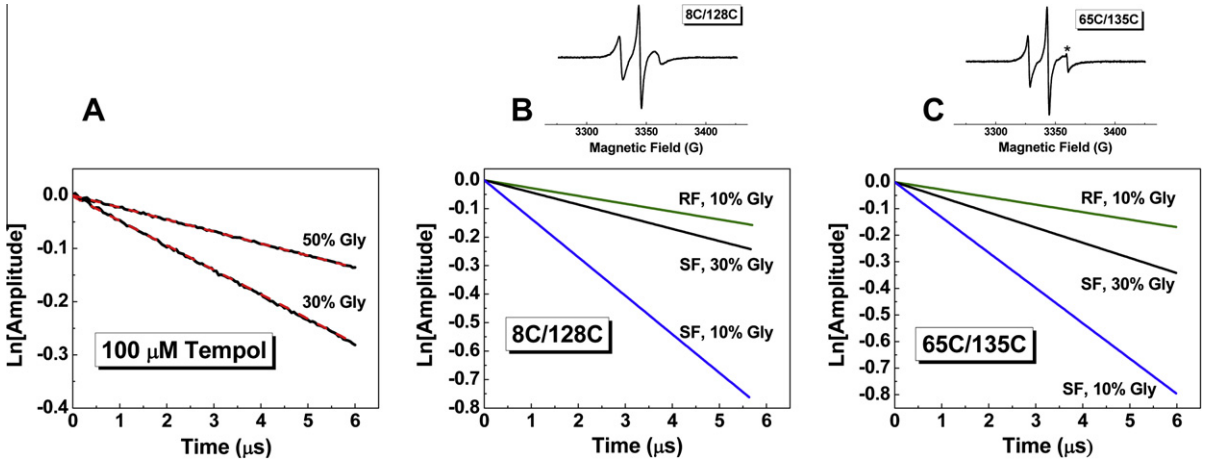

Fig. 4. This figure provides the DEER background signals in logarithm scale for samples of 100 μM Tempol and doubly spin-labeled mutants of T4L both slow frozen: Panel A shows the experimental DEER signals in logarithm scale for samples with 100 μM Tempol in 30% and 50% Gly-d8/D_2O (in black) and their linear fits (in red). Panel B shows the homogeneous background of the DEER signals for samples of doubly spin-labeled T4L mutant 8C/128C prepared by rapid freezing (in green) in 10% glycerol, slow (regular) freezing in 30% glycerol (in black) and slow (regular) freezing in 10% glycerol (in blue). Panel C shows the homogeneous background of the DEER signals for samples of doubly spin-labeled T4L mutant 65C/135C prepared by rapid freezing in 10% glycerol (in green), slow (regular) freezing in 30% glycerol (in black) and slow (regular) freezing in 10% glycerol (in blue). For the clarity of presentation, all background signals were normalized to unity in the original echo-amplitude scale. The CW ESR spectra of spin-labeled double cysteine mutants 8C/128C and 65C/135C in 10% glycerol at RT are shown in panels B and C. As seen, the contribution of free spin-label to the CW ESR spectrum (designated by asterisk in panel C) and consequently to the background in DEER signals is insignificant.

8C/44C, 8C/128C, and 65C/135C, with the 4-Bromo derivative of MTSL. The samples were regularly shock-frozen in liquid N_2 and contained 30% Glycerol. The time-domain DEER data and distance distributions for doubly spin-labeled with MTSL (green) and

4-Bromo MTSL (orange) are compared in Fig. 5. Indeed, the two spin-labels produced somewhat different time-domain DEER signals and distance distributions, which we believe reflect different populations of side chain rotamers. In general the distance distributions from 4-Bromo MTSL were narrower. Interestingly, in the case of mutant 8C/128C spin-labeled with 4-Bromo MTSL a single peak distribution was obtained, which coincides with the peak at 4 nm in the bimodal distance distribution using MTSL.

4. Discussion

4.1. Implications of the sample freezing rate on distance distributions: contributions from tether rotamers and/or protein conformations

Our initial objective was to determine the perturbation on the protein structure due to freezing conditions since this perturbation could affect the interpretation of the results from DEER measurements. Therefore, we conducted experiments on samples which were frozen at three substantially different freezing rates: rapidly (within 100 μs), slowly (within 1 s) and very slowly (within 30–40 s). Our results show the distance maxima between studied spin-labeled sites are in general unchanged, regardless of the freezing method (rate) used.

Compared to slowly frozen samples, the rapidly frozen samples showed broadened inter bi-label distance distributions for all the double mutants studied. The logical assumption is that with rapid freezing a larger ensemble, including higher energy states, of spin label, possibly including protein conformers is rapidly trapped. Since one studies frozen samples at cryogenic temperature, the contribution from the dynamical properties of the spin-label and/or protein is limited by the freezing times, which determine the capacity of the system to relax to the lowest energy microstates at temperatures of liquid N_2. The shortest freezing time in our experiments was $\leqslant$100 μs. This puts a 100 μs upper limit on the time for conformers and rotamers to find the available lowest energy microstates on the energy landscape. This landscape is provided by the system, which is the protein, and by nearby, protein-coupled solvent. Of relevance to the nature of that solvent is the likelihood that rapidly frozen samples [32], including those like ours prepared by spraying onto a cold metal surface below 130 K [26], consist of amorphous ice, a solid that exhibits a disordered liquid-like arrangement [33]. If our rapidly frozen sample consists of amorphous ice, then the protein side chains and spin label tethers appear to have been frozen in a disordered state without the time to search the protein-solvent landscape for energy minima. Slower freezing with a longer time at the freezing point should enable the protein, the label, and the protein-coupled solvent to achieve a reduced number of well resolved energy minima. Indeed, the slowest frozen samples showed a distance distribution with sharpest peaks, but fewer features.

It was interesting to determine whether, in our experiment, we could trap both spin-label and protein conformers, which are possibly affected by the sample freezing rate, and to distinguish their relative contributions to our experimentally obtained distance distributions. Recently, an NMR study on L99A T4L reported co-existence in solution of a stable long lived conformation and a transient, much less populated, conformation with life time of about 1 ms [34]. Protein plasticity as a prerequisite for functionality has emerged as a general idea in protein science [34,35]. Therefore multiple approaches and methods to characterize these states

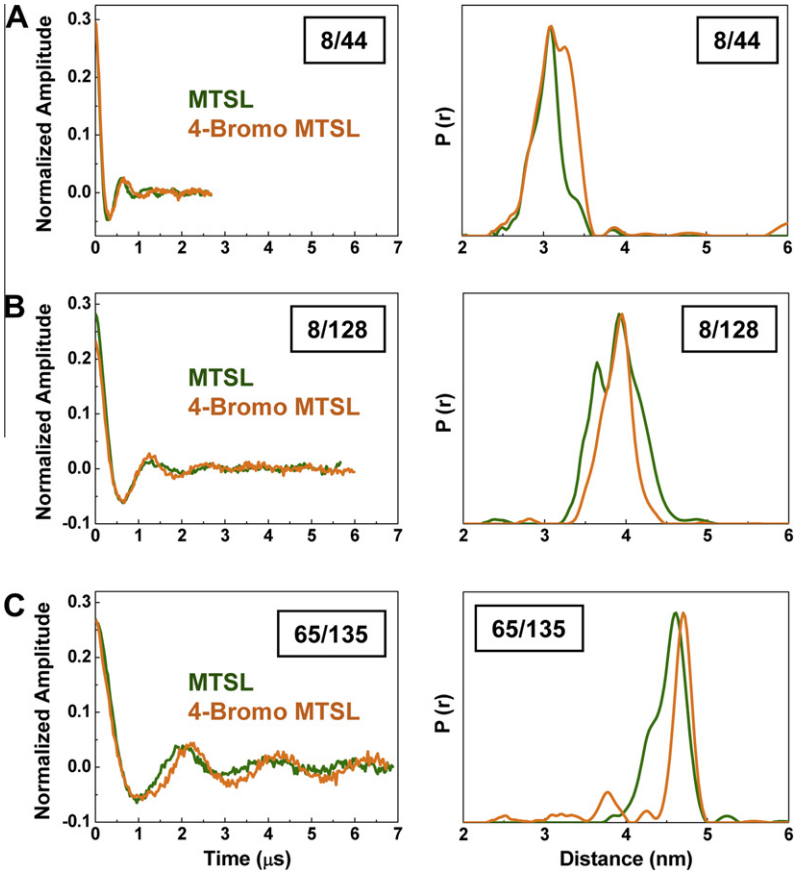

Fig. 5. This figure provides experimental base-line corrected and normalized DEER signals and reconstructed distances and distance distributions for T4L mutants 8/44 (panel A), 8/128 (panel B), 65C/135C (panel C) spin-labeled with MTSL (green) and 4-Bromo MTSL (orange) are shown. The samples were regularly shock-frozen in liquid N_2 and contain 30% glycerol. The distance distributions are normalized in arbitrary units to unity at maximum intensity.

are necessary. However, our experiments with 4-Bromo MTSL have implied that tether rotamers contribute significantly to the observed distance distributions. 4-Bromo substituted MTSL was used previously in a study of T4L at physiological temperatures and it was found that this spin-label has more restricted mobility when compared to MTSL due to restricted amplitude of internal bond rotations in the side chain [12]. Therefore the expectation was to obtain narrower distance distributions when using 4-Bromo MTSL instead of MTSL, and this expectation was in general agreement with our results. To further help in understanding the origin of our observed distance distributions, we performed an additional analysis by using molecular modeling software (MMM) [13] which predicts possible weighted rotamers of MTSL, and consequently distance distributions, based on force fields and existing structures at atomic resolution. A large number of rotamers was calculated for each solvent exposed spin-labeled residue of T4L yielding distance distributions between each pair of spin-labeled residues that are complex. The resolution of the calculated distance distributions was insufficient to distinguish contributions from protein conformations (Supplementary data).

4.2. Dependence of DEER signal on glycerol content and sample freezing rate

Rapid freeze-quench allows for the possibility of trapping high energy rotamers of the spin label (and possibly protein conformers, if the resolution of the experiment allows) and thereby to report on properties of the system at higher temperatures corresponding to more physiological conditions. Also we noticed a reduction of the background signal of the DEER experimental data for rapidly frozen samples when compared with the samples prepared by slow freezing in liquid N_2. This background signal is produced mainly by the mechanism of instantaneous spin diffusion due to spin–spin interactions with neighboring spin-labeled molecules and therefore depends on the effective local spin concentration [22,31]. Therefore we concluded that rapid freezing provides a more uniform (isotropic) distribution of spin-labeled molecules within the sample volume thereby reducing the contribution of inter-molecular spin–spin interactions to the DEER signal. This increases the phase memory relaxation times (T_m's) and also facilitates the data analysis. For samples of a small globular protein like T4L in 30% glycerol prepared by slow freezing in liquid N_2 the slope of the background DEER time-domain signal, resulting from the effective local spin-concentration, increases by about a factor of 1.5–2 when compared to the bulk spin concentration. However, this increase is about a factor of 5–6 for samples containing 10% glycerol and prepared by slow freezing (Fig. 3, left-most panel, Fig. 5), indicating high local spin-concentration due to insufficient glycerol/water vitrification and protein aggregation. The direct implication of the latter effect on the DEER data is shortened T_m's, resulting in lower SNR of the time-domain signals, insufficient time for signal evolution, and reduced resolution of reconstructed distances.

The amount of glycerol used in biological samples for low temperature ESR is highly empirical, and one should, in general, avoid using too high a concentration of glycerol, since there is risk of modifying the properties of proteins, for example their solvation and dynamic behavior [36,37] Our results here clearly show that samples containing sufficiently homogeneous distributed bi-spin labeled protein molecules can be achieved at low glycerol concentration, as small as 10%, when rapid freezing is used.

5. Conclusions

We used bi-spin labeled T4L mutants prepared at different freezing rates and with different concentrations of vitrifying glycerol cryoprotectant to study freezing-induced perturbations on the distance distributions derived from DEER. Results of note were:

(i) The freezing rate alters the distance distribution, most likely because trapping of spin-label conformational substates depends on the rate of freezing. Rapid freezing ($\leqslant$100 μs) provides a broadened distribution; slow freezing ($\geq$1 s) showed better resolved and narrower features.
(ii) No difference was observed in the mean interprobe distance from the same mutant, regardless of freezing rate or cryoprotectant percentage, which suggests that the freezing of protein samples for study at low temperatures does not perturb the structure significantly.
(iii) Slow freezing with higher cryoprotectant (30% glycerol) or rapid freeze-quench done at 10% glycerol both provided samples having a distribution of spin-labeled biological molecules/complexes with long phase memory times, reduced intermolecular spin–spin interactions, and good DEER SNR.
(iv) The use of the Bromo-substituted MTSL typically leads to narrower distance distributions probably because of fewer low-energy rotamers and is helpful to distinguish when bimodal distance distributions result from rotamers of unsubstituted MTSL.

Acknowledgments

J. H. Freed, E. R. Georgieva, A. S. Roy, and P. P. Borbat acknowledge financial support from NIH/NCRR Grant P41RR016292. C. P. Scholes and V. M. Grigoryants acknowledge financial support from NIH Grants 3RO1GM06625304S1 and RO1 GM066253-01A1. K. A. Earle acknowledges support from an RNA Institute Interdisciplinary Pilot Research Program 2010 Award, UAlbany. AddGene is acknowledged for the plasmid of T4L and Dr. Cynthia Kinsland, Protein Facility of Cornell University, is acknowledged for advices in mutagenesis. T4L mutants were expressed in the Protein Facility of Cornell University.

Appendix A. Supplementary material

Supplementary data associated with this article can be found, in the online version, at doi:10.1016/j.jmr.2012.01.004.

References

[1] W.L. Hubbell, D.S. Cafiso, C. Altenbach, Identifying conformational changes with site-directed spin labeling, Nat. Struct. Biol. 7 (2000) 735–739.
[2] P.P. Borbat, J.H. Freed, Pros and cons of pulse dipolar ESR: DQC and DEER, EPR Newsl. 17 (2007) 21–33.
[3] G. Jeschke, Y. Polyhach, Distance measurements on spin-labelled biomacromolecules by pulsed electron paramagnetic resonance, Phys. Chem. Chem. Phys. 9 (2007) 1895–1910.
[4] O. Schiemann, T.F. Prisner, Long-range distance determinations in biomacromolecules by EPR spectroscopy, Q. Rev. Biophys. 40 (2007) 1–53.
[5] Y.W. Chiang, P.P. Borbat, J.H. Freed, The determination of pair distance distributions by pulsed ESR using Tikhonov regularization, J. Magn. Reson. 172 (2005) 279–295.
[6] Y.W. Chiang, P.P. Borbat, J.H. Freed, Maximum entropy: a complement to Tikhonov regularization for determination of pair distance distributions by pulsed ESR, J. Magn. Reson. 177 (2005) 184–196.
[7] E.R. Georgieva, T.F. Ramlall, P.P. Borbat, J.H. Freed, D. Eliezer, Membrane-bound alpha-synuclein forms an extended helix: long-distance pulsed ESR measurements using vesicles, bicelles, and rodlike micelles, J. Am. Chem. Soc. 130 (2008) 12856–12857.
[8] E.R. Georgieva, T.F. Ramlall, P.P. Borbat, J.H. Freed, D. Eliezer, The lipid-binding domain of wild type and mutant alpha-synuclein: compactness and interconversion between the broken and extended helix forms, J. Biol. Chem. 285 (2010) 28261–28274.
[9] S.Y. Park, P.P. Borbat, G. Gonzalez-Bonet, J. Bhatnagar, A.M. Pollard, J.H. Freed, A.M. Bilwes, B.R. Crane, Reconstruction of the chemotaxis receptor-kinase assembly, Nat. Struct. Mol. Biol. 13 (2006) 400–407.

[10] J. Bhatnagar, J.H. Freed, B.R. Crane, Rigid body refinement of protein complexes with long-range distance restraints from pulsed dipolar ESR, Methods Enzymol. 423 (2007) 117–133.
[11] J. Bhatnagar, P.P. Borbat, A.M. Pollard, A.M. Bilwes, J.H. Freed, B.R. Crane, Structure of the ternary complex formed by a chemotaxis receptor signaling domain, the CheA histidine kinase, and the coupling protein CheW as determined by pulsed dipolar ESR spectroscopy, Biochemistry 49 (2010) 3824–3841.
[12] C. Altenbach, K.J. Oh, R.J. Trabanino, K. Hideg, W.L. Hubbell, Estimation of inter-residue distances in spin labeled proteins at physiological temperatures: experimental strategies and practical limitations, Biochemistry 40 (2001) 15471–15482.
[13] Y. Polyhach, E. Bordignon, G. Jeschke, Rotamer libraries of spin labelled cysteines for protein studies, Phys. Chem. Chem. Phys. 13 (2011) 2356–2366.
[14] W.A. Baase, L. Liu, D.E. Tronrud, B.W. Matthews, Lessons from the lysozyme of phage T4, Protein Sci. 19 (2010) 631–641.
[15] L. Columbus, T. Kalai, J. Jeko, K. Hideg, W.L. Hubbell, Molecular motion of spin labeled side chains in alpha-helices: analysis by variation of side chain structure, Biochemistry 40 (2001) 3828–3846.
[16] L. Columbus, W.L. Hubbell, A new spin on protein dynamics, Trends Biochem. Sci. 27 (2002) 288–295.
[17] Z. Zhang, M.R. Fleissner, D.S. Tipikin, Z. Liang, J.K. Moscicki, K.A. Earle, W.L. Hubbell, J.H. Freed, Multifrequency electron spin resonance study of the dynamics of spin labeled T4 lysozyme, J. Phys. Chem. B 114 (2010) 5503–5521.
[18] P.P. Borbat, H.S. McHaourab, J.H. Freed, Protein structure determination using long-distance constraints from double-quantum coherence ESR: study of T4 lysozyme, J. Am. Chem. Soc. 124 (2002) 5304–5314.
[19] M. Matsumura, J.A. Wozniak, D.P. Sun, B.W. Matthews, Structural studies of mutants of T4 lysozyme that alter hydrophobic stabilization, J. Biol. Chem. 264 (1989) 16059–16066.
[20] M. Matsumura, Control of enzyme activity by an engineered disulfide bond, Science 243 (1989) 792–994.
[21] P.P. Borbat, R.H. Crepeau, J.H. Freed, Multifrequency two-dimensional Fourier transform ESR: an X/Ku-band spectrometer, J. Magn. Reson. 127 (1997) 155–167.
[22] P.P. Borbat, J.H. Freed, Measuring distances by pulsed dipolar ESR spectroscopy: spin-labeled histidine kinases, Methods Enzymol. 423 (2007) 52–116.
[23] Y. Lin, G.J. Gerfen, D.L. Rousseau, S.-R. Yeh, Ultrafast microfluidic mixer and freeze-quenching device, Anal. Chem. 75 (2003) 5381–5386.
[24] V.M. Grigoryants, C.P. Scholes, Variable velocity liquid flow EPR and submillisecond protein folding (Chapt. 5.3), in: V.N. Uversky, E.A. Permyakov (Eds.), Protein Structures: Methods in Protein Structure and Stability Analysis, Nova Science Publishers, Inc., New York, 2006, pp. 47–71.
[25] V.M. Grigoryants, A.V. Veselov, C.P. Scholes, Variable velocity liquid flow EPR applied to submillisecond protein folding, Biophys. J. 78 (2000) 2702–2708.
[26] F.G.M. Wertz, Electron transfer and proton pumping pathways in cytochrome aa_3, in: Dept. of Biotechnology, Delft University of Technology, Delft, Netherlands, 2008, pp 41–60 (Chapter 2).
[27] B. Schmidt, G. Mahmud, S. Soh, S.H. Kim, T. Page, T.V. O'Halloran, B.A. Grzybowski, B.M. Hoffman, Design, implementation, simulation, and visualization of a highly efficient RIM microfluidic mixer for rapid freeze-quench of biological samples, Appl. Magn. Reson. 40 (2011) 415–425.
[28] W.B. Bald, The relative merits of various cooling methods, J. Micros. 140 (1985) 17–40.
[29] G.J. Jones, On estimating freezing times during tissue rapid freezing, J. Micros. 136 (1984) 349–360.
[30] A.D. Milov, R.I. Samoilova, Y.D. Tsvetkov, C. Peggion, F. Formaggio, C. Toniolo, J. Raap, Aggregation of spin-labeled alamethicin in low-polarity solutions as studied by PELDOR spectroscopy, Dokl. Phys. Chem. 406 (2006) 21–25.
[31] A.M. Raitsimring, K.M. Salikhov, B.A. Umanskii, Y.D. Tsvetkov, Instantaneous diffusion in electron-spin echo of paramagnetic centers stabilized in solid matrices, Fiz. Tverd. Tela+ 16 (1974) 756–766.
[32] A.V. Cherepanov, S. De Vries, Microsecond freeze-hyperquenching: development of a new ultrafast micro-mixing and sampling technology and application to enzyme catalysis, Biochim. Biophys. Acta 1656 (2004) 1–31.
[33] O. Mishima, H.E. Stanley, The relationship between liquid, supercooled and glassy water, Nature 396 (1998) 329–335.
[34] G. Bouvignies, P. Vallurupalli, D.F. Hansen, B.E. Correia, O. Lange, A. Bah, R.M. Vernon, F.W. Dahlquist, D. Baker, L.E. Kay, Solution structure of a minor and transiently formed state of a T4 lysozyme mutant, Nature 477 (2011) 111–114.
[35] N. Tokuriki, D.S. Tawfik, Protein dynamism and evolvability, Science 324 (2009) 203–207.
[36] R. Sinibaldi, M.G. Ortore, F. Spinozzi, F. Carsughi, H. Frielinghaus, S. Cinelli, G. Onori, P. Mariani, Preferential hydration of lysozyme in water/glycerol mixtures: A small-angle neutron scattering study, J. Chem. Phys. 126 (2007) 235101–235109.
[37] A. Paciaroni, S. Cinelli, G. Onori, Effect of the environment on the protein dynamical transition: a neutron scattering study, Biophys. J. 83 (2002) 1157–1164.